Pakistan Veterinary Journal

ISSN: 0253-8318 (PRINT), 2074-7764 (ONLINE)
DOI: 10.29261/pakvetj/2025.194

RESEARCH ARTICLE

Cis-9, Trans-11 Conjugated Linoleic Acid Promotes Apoptosis, Restores Oxidative Homeostasis and Inhibits the Proliferation of Canine Mammary Tumor Cells

Yuquan Ren[1], Zihan Wang[1], Meng Li* and Xiangzhen Shen*

College of Veterinary Medicine, Nanjing Agricultural University, Nanjing 210095, P. R. China. # Yuquan Ren and Zihan Wang contributed equally to this work.
*Corresponding author: limeng@njau.edu.cn; xzshen@njau.edu.cn

ARTICLE HISTORY (25-098)

Received: February 6, 2025
Revised: May 22, 2025
Accepted: June 3, 2025
Published online:

Key words:
Antioxidation
Apoptosis
Canine mammary tumors
Conjugated linoleic acid

A B S T R A C T

Canine mammary tumors (CMTs), one of the most common malignant neoplasms in female dogs, currently lack effective chemotherapeutic options beyond surgical treatment. Conjugated linoleic acid (CLA), particularly the cis-9, trans-11 CLA (c9, t11-CLA) isomer, has demonstrated anticancer potential in human studies; however, its specific mechanisms in CMTs remain largely unexplored. This study investigated the antitumor effects of c9, t11-CLA on the CMT cell line CMT-U27, focusing on apoptosis regulation and oxidative stress modulation, thereby providing the theoretical basis for developing novel anti-tumor therapies. Following treatment of the CMT-U27 cells with various concentrations of c9, t11-CLA, CCK-8 assays revealed a concentration-dependent increase in apoptosis. Quantitative RT-qPCR and western blot analyses were performed to assess the 120μM, the expression of the anti-apoptotic proteins (Bcl-2 and Bcl-XL) was significantly decreased ($P<0.05$), while the expression of proapoptotic proteins (Bax and Bad) increased ($P<0.05$). Additionally, catalase expression was reduced ($P<0.05$), the malondialdehyde content was increased, and superoxide dismutase activity was decreased. In summary, this study demonstrates that c9, t11-CLA treatment significantly inhibits the proliferation of CMT-U27 cells, potentially through modulation of Bcl-2 family protein expression, activation of peroxisome proliferator-activated receptor gamma (PPARγ), and disruption of the oxidative homeostasis.

To Cite This Article: Ren y, Wang Z, Li M and Shen X 2025. Cis-9, Trans-11 conjugated linoleic acid promotes apoptosis, restores oxidative homeostasis, and inhibits the proliferation of canine mammary tumor cells. Pak Vet J, 45(2): 807-815. http://dx.doi.org/10.29261/pakvetj/2025.194

INTRODUCTION

Canine mammary tumors (CMTs) are the most prevalent neoplastic disease affecting intact aged female dogs (Kristiansen *et al*., 2016), during which 35%–50% of CMTs are malignant, resulting in a high percentage of mortality. However, no ideal chemotherapy method exists to reduce the recurrence and metastasis of CMTs, while surgical resection is the commonly used treatment approach (Sleeckx *et al*., 2011). Despite their clinical significance, the molecular mechanisms driving CMTs' progression remain poorly understood. The pathogenesis of CMTs is predominantly influenced by endogenous ovarian hormone exposure (Tamarindo *et al*., 2023), while additional factors such as obesity, inflammation, and excessive free radicals and reactive oxygen species (ROS) are the secondary contributing factors (Machado *et al*., 2015). Recent research showed that *homoharringtonine* inhibits p-AKT/p-mTOR by inducing mitochondrial apoptosis, and dual ERβ agonism disrupts ERα-PI3K/AKT axis in CMTs, offering hormone-targeted therapies and immunotherapy to improve outcomes in canine oncology (Mei *et al*., 2024; Yoo *et al*., 2024). However, research on ROS-related mechanisms remains insufficient. Extensive evidence highlights significant similarities between CMTs and human breast cancer in terms of disease presentation, histopathological features, biological behavior, and metastatic patterns (Belury, 2002). Consequently, CMTs have emerged as a pivotal spontaneous model for evaluating novel anticancer therapies. Advancements in the clinical management of CMTs may contribute to developing improved treatment strategies, ultimately optimizing outcomes in both veterinary and human oncology.

Conjugated linoleic acid (CLA) is primarily found in milk, dairy products, and meat from ruminants. In the rumen, CLA is synthesized through biohydrogenation, during which ruminal microorganisms convert linoleic acid

into stearic acid via the formation of CLA. In addition to rumen bacteria, *Propionibacterium* and *Bifidobacterium* can also produce CLA (Iorizzo *et al*., 2024). CLA has attracted considerable attention due to its antihypertensive, anti-inflammatory, antidiabetic, immunomodulatory, and anticancer effects (Ma *et al*., 2019; Poleti *et al*., 2020; Zeng *et al*., 2020; Chen *et al*., 2024; Wu *et al*., 2024). In colorectal cancer (CRC), CLA has been shown to exert protective effects by modulating cytokine production, inhibiting the NF-κB signaling pathway, and regulating gut microbiota through a PPAR-γ-dependent manner (Ngema *et al*., 2023). Additionally, dietary c9, t11-CLA enriched from butter has demonstrated preventive effects against breast cancer by inhibiting hormonal receptors and suppressing cell proliferation (Zeng *et al*., 2020). Cis-9, trans-11-CLA (c9, t11-CLA), as the primary CLA isomer in bovine milk lipids, accounts for approximately 80–90% of the total CLA content, whereas trans-10, cis-12 CLA isomer represents only 1% (Jensen *et al*., 2000).

Although numerous in vivo studies have confirmed the antitumor properties of CLA across various animal models, the underlying molecular mechanism remains unclear. Early clinical evidence suggested that CLA inhibits the initiation and growth of mammary, lung, colon, and gastric tumors through diverse pathways, including the modulation of eicosanoid metabolism, induction of lipid peroxidation and regulation of genes controlling cellular proliferation, and apoptosis (Kilian *et al*., 2002; Lu *et al*., 2015). Additionally, the mechanism by which CLA inhibits carcinogenesis appears to differ depending on tumor types, developmental stages, and organs (Park *et al*., 2001), involving alterations in cell proliferation, immune response modulation, lipid metabolism, and gene expression (Belury, 2002). Specifically, El Roz *et al.* (2013) showed that CLA can inhibit the development of early gastric tumors through the induction of lipid peroxidation in mouse models. Fite *et al*. (2007) found[0] that CLA can inhibit the formation of lung cancer and reduce the production of eicosanoids through lipid metabolism. Wang *et al*. (2006) demonstrated that CLA can disrupt the normal operation cycle of colon cancer cells, thereby suppressing the growth of malignant tumor cells.

Furthermore, Da Silva *et al*. (2023) demonstrated that c9, t11-CLA stimulates apoptotic genes in tubular and papillary carcinoma of the breast but exerts the opposite effect in anaplastic carcinoma. Another study also showed that CLA intake may attenuate aluminum chloride-induced apoptosis by modulating the expression of apoptosis-related proteins (Cuciniello *et al*., 2024). While CLA has demonstrated antitumor effects in human breast cancer through PPARγ activation and oxidative stress modulation (Belury, 2002), its role in CMTs is virtually unexplored.

Thus, c9, t11-CLA acts as a new potential drug choice and presents a theoretical basis for treating CMTs. This study explored the antitumor mechanism of c9, t11-CLA in CMT-U27 cells, particularly its effects on apoptosis-related gene expression, PPARγ activation, and oxidative stress modulation.

MATERIALS AND METHODS

Ethics statement: The Institutional Animal Care and Use Committee of Nanjing Agricultural University approved the experimental design, and all procedures adhered strictly to the "Guidelines for Experimental Animals" of the Ministry of Science and Technology (2006, Beijing, China).

Cell culture: CMT-U27 (CRL-3456) (ATCC) cells were cultured in complete medium containing 90% RPMI medium 1,640 basic (1×), penicillin (100U/mL), streptomycin (0.1mg/mL) (Solarbio, Beijing, China), and 10% fetal bovine serum (Zeta Life, California, USA). The typical cell morphology of the cultured cells is shown in Figure. 1(A).

Cytotoxicity assay: CMT-U27 cells were cultured overnight in a 96-well plate, treated with configured C9, t11-CLA ($C_{18}H_{32}O_2$; 90%, >100mg) (MATREYA LLCCL) at different concentrations (0, 10, 50, 100, 500, or 1,000μM) for 48h, and then incubated with 10μL of Cell Counting Kit-8 (CCK-8) (Biosharp Life Sciences) reagent solution for 1h. Absorbance was measured at 450nm using a microplate reader (Thermo Fisher Scientific Inc., Waltham, MA, USA). Cell viability was evaluated based on the measured OD values.

Real-Time quantitative Polymerase Chain Reaction (PCR): Total RNA from cells was extracted using Trizol reagent (Catalog No. 9108, Takara, China). The concentration of RNA in each sample was detected using a spectrophotometer (Thermo Fisher Scientific Inc., Waltham, Massachusetts, USA). Complementary cDNA was synthesized using the HiScript® III RT SuperMix (Vazyme Biotech, Nanjing) for the qPCR kit following the manufacturer's instructions. The relevant primers were designed using the Oligo7 software, commercially synthesized by Sangon Biotech (Shanghai), with sequences listed in Table 1. Each sample was evaluated using the Cham Q Universal SYBR qPCR Master Mix kit (Vazyme Biotech, Nanjing) for PCR amplification. GAPDH was used as the standard control, and results were quantified using the $2^{-\Delta\Delta Ct}$ method.

Western Blot analysis: Total cellular proteins were extracted using RIPA buffer (Solarbio, Beijing, China) with 1% PMSF (Beyotime Biotechnology, Shanghai, China), after which the protein concentration was measured using the BCA protein quantification kit (Yamei Biomedical Technology, Shanghai). Subsequently, 10μL of protein samples were separated by 10% SDS polyacrylamide gel electrophoresis and transferred onto polyvinylidene fluoride membranes (Yamei Biomedical Technology, Shanghai). Membranes were blocked at RT for 2h with 7% skim milk, followed by overnight incubation with the corresponding primary antibody at 4°C. After washing with TBST, membranes were incubated with secondary antibodies at RT for 2h. To detect the target protein, the bands were incubated with chemiluminescent solution using the Basic Chemiluminescence Detection Kit (Yamei Biomedical Technology, Shanghai), and results were analyzed using the Image Lab software (Bio-rad, Berkeley, CA, USA).

The following antibodies were used for western blotting: Bax (1:1,000; CY6717, Abways, Shanghai, China), Bcl-2 (1:1,000; CY5059, Abways, Shanghai,

Table 1: Nucleotide sequence of the primers used in relevant analysis

Gene	Forward primer (5'-3')	Reverse primer (5'-3')	Length/ bp
GAPDH	GTCGCCATCAATGACCCCTT	ATGGACTTCCCGTTGATGACA	131
Bax	ATCCACCAAGAAGCTGAGCGAA	GCGATCATCCTCTGCAACTCCA	81
Bcl-2	CGACTTCTCCCGCCGCTACCG	ACCGTGGCAAAGCGTCCCCTC	93
Bcl-XL	CTGAATGACCACCTAGAGCCTT	ACACCAGCCACAGTCATGC	149
Bad	ACTTCCTCGCCCGAAGAGC	CCTCCTCTCCCCAAGTTCCGAT	105
Caspase3	TAAAAGTACTGGAATGGCAC	TTCCAAAATTTCTTCGCAT	127
PPARγ	CATTCTCAAGAGCGGACCC	GCTCCACTTTGATTGCACT	84
CAT	TCACTCAGGTGCGGACTTTC	TGGATGCGGGAGCCATATTC	163

China), β-actin (1:1000; #4970, CST, Massachusetts, USA), and HRP-conjugated goat anti-rabbit IgG (H+L) secondary antibody (1:5,000; SA00001, PTG, Chicago, USA).

Evaluation of MPO and SOD activities: Myeloperoxidase (MPO) and total superoxide dismutase (SOD) activities were detected according to instructions of the respective assay kits (Jiancheng Bioengineering Institute, Nanjing).

Statistical analysis: Statistical analysis was performed using IBM SPSS Statistics 21 for one-way analysis of variance, followed by the LSD post-hoc test. All data were presented as mean±SEM. Graphs were plotted using GraphPad Prism 8. Significant levels were set at *P<0.05 and **P<0.01 to indicate significant and extremely significant differences, respectively.

RESULTS

Proliferation toxicity of c9, t11-CLA on CMT cells: Figure. 1(B) shows the results of the CCK8 test. After c9, t11-CLA acts on CMT-U27 cells for 48h, and the cell activity is reduced. At the concentration of < 120μM, the result showed the activity of CMT-U27 remained unaltered with no significant changes, whereas at ≥ 120μM, the cell activity decreased significantly. Statistical analysis using the SPSS software revealed highly significant differences (P<0.01) in cellular activity between the treatment groups (120, 150, and 180μM) and the control group, with the growth inhibition proportions being 89.04, 87.56, and 82.61%, respectively.

As illustrated in Figure. 1(C), after c9, t11-CLA acts on CMTs for 48h, the cell growth inhibition rate increased significantly. At concentrations of 30, 60, and 90μM, the inhibitory effect of CLA on cells showed no significant increases, with the inhibition rates being 0.53, 0.79, and 4.38%, respectively. At concentrations ≥ 120μM, the inhibition rate increased significantly, showing highly substantial variations from the control group (P<0.01), indicating that CLA exerts a pronounced inhibitory effect on the proliferation of CMT cells.

Morphological changes in CMT cells induced by c9, t11-CLA: CMT-U27 cells in the normal morphological state are arranged in a fascicular pattern, displaying vigorous proliferation with clear cell boundaries, strong adhesion, high refractility, and a polygonal or spindle-shaped morphology (Fig. 1-D). After the action of 60μM c9, t11-CLA for 48h, the cells retained good viability with no significant morphological alterations (Fig. 1-E). Cell morphology progressively deteriorated with increasing c9, t11-CLA concentrations. At 120μM, the adherent ability of the cells weakened, the number of adherent cells reduced, oval-shaped cells appeared, the refractivity became poor, and boundaries became indistinct (Fig. 1-F). At 180μM, the number of adherent cells decreased significantly, the cells shrank, and obvious cell debris and necrotic cells were detected in the visual field (Fig. 1-G). Hence, after c9, t11-CLA acts on cells for 48h, the cell state worsens, and the apoptotic morphology becomes increasingly evident with the increase in concentration.

Analysis of apoptosis modulation in CMT-U27 cells by c9, t11-CLA by RT-qPCR: Figure. 2 presents the results of the fluorescence quantitative test. After treating CMT-U27 cells with c9, t11-CLA, the expression of the apoptotic regulatory genes Bcl-2 and Bcl-XL changed significantly in comparison to those in the control group. At a c9, t11-CLA concentration of 60μM, the expression of Bcl-2 and Bcl-XL shows a slight downregulation (P>0.05). At ≥ 120μM, both proteins showed significant downregulation (P<0.05), with the expression of Bcl-XL decreased significantly at 180μM (P<0.01) (Fig. 2- A, B). Conversely, the expression of the proapoptotic genes Bax and Bad exhibited significant upregulation at higher concentrations. At 60μM, the results showed no significant changes in Bax or Bad expression. At 120μM, an increased expression of Bax has been shown (P<0.05), whereas the Bad expression remained unchanged. In contrast to the control group, both Bax and Bad expression demonstrated highly significant differences at 180μM (P<0.01) (Fig. 2-C, D).

To further elucidate the molecular mechanisms behind c9, t11-CLA's antiapoptotic function, the mRNA expression of PPARγ was detected using different concentrations (60, 120, and 180μM) of c9, t11-CLA for CMTs. The transcriptional activity of PPARγ, which is closely associated with apoptosis, exhibited an increasingly inhibitory effect observed at higher concentrations, with a significant increase at 180μM (P<0.05). This trend parallels the expression pattern of caspase-3 (Fig. 2-E, F).

Expression changes in regulating apoptosis proteins analyzed using Western Blotting: The results of Western blotting are presented in Fig. 3. Once the CMT-U27 cells were subjected to c9,t11-CLA, the results showed an increased expression of Bax, and that of the anti-apoptotic protein Bcl-2 decreased relative to the control group. At 60μM, the expression of Bcl-2 showed no significant change and displayed a slight increase. At ≥ 120μM, the expression of Bax was significantly upregulated (P<0.01), concomitant with a marked reduction in Bcl-2 expression (P<0.05). Notably, at 180μM, the expression of Bcl-2 decreased significantly (P<0.01). We detected the ratio of Bax/Bcl-2 expression and observed that it showed no

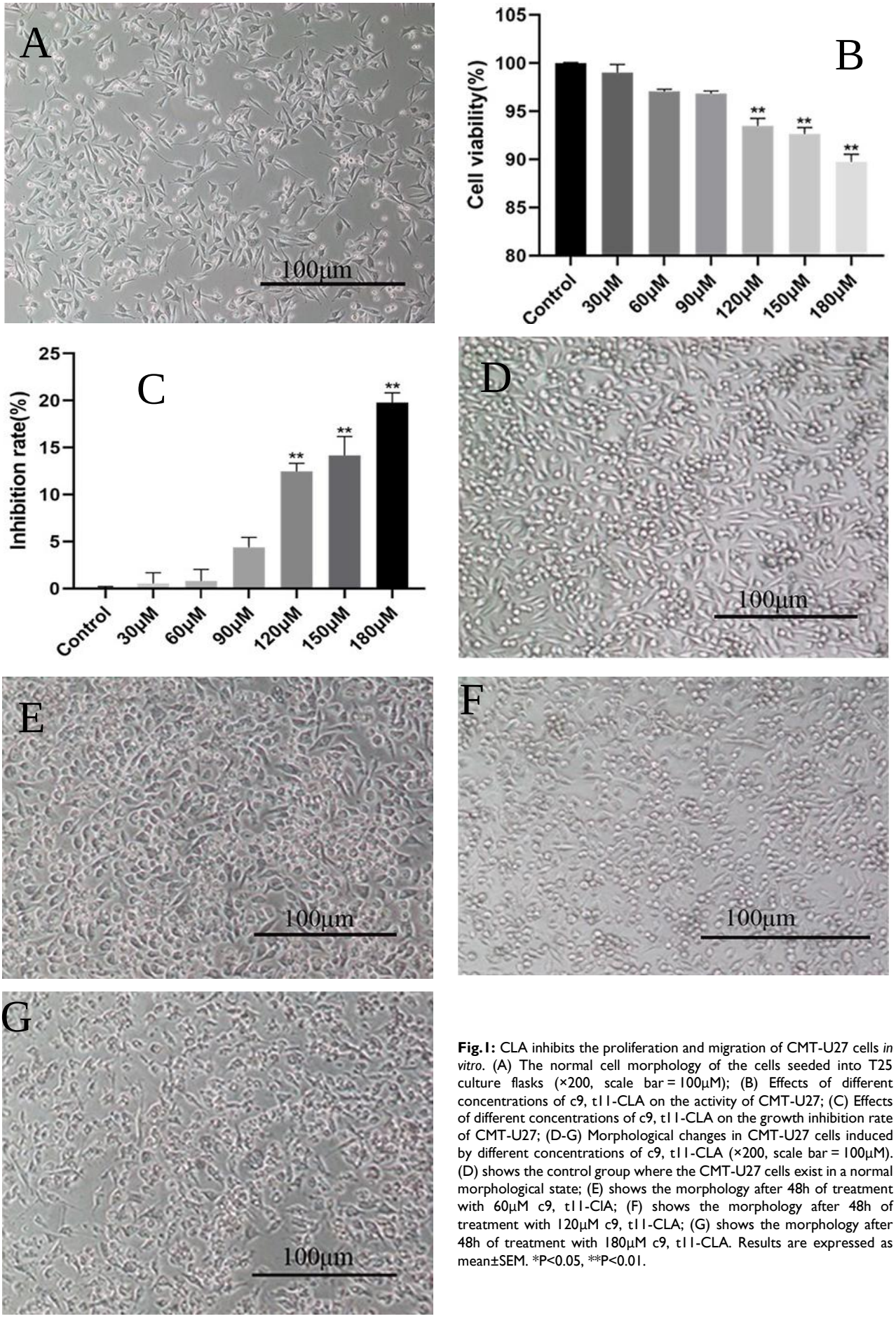

Fig.1: CLA inhibits the proliferation and migration of CMT-U27 cells *in vitro*. (A) The normal cell morphology of the cells seeded into T25 culture flasks (×200, scale bar = 100μM); (B) Effects of different concentrations of c9, t11-CLA on the activity of CMT-U27; (C) Effects of different concentrations of c9, t11-CLA on the growth inhibition rate of CMT-U27; (D-G) Morphological changes in CMT-U27 cells induced by different concentrations of c9, t11-CLA (×200, scale bar = 100μM). (D) shows the control group where the CMT-U27 cells exist in a normal morphological state; (E) shows the morphology after 48h of treatment with 60μM c9, t11-ClA; (F) shows the morphology after 48h of treatment with 120μM c9, t11-CLA; (G) shows the morphology after 48h of treatment with 180μM c9, t11-CLA. Results are expressed as mean±SEM. *P<0.05, **P<0.01.

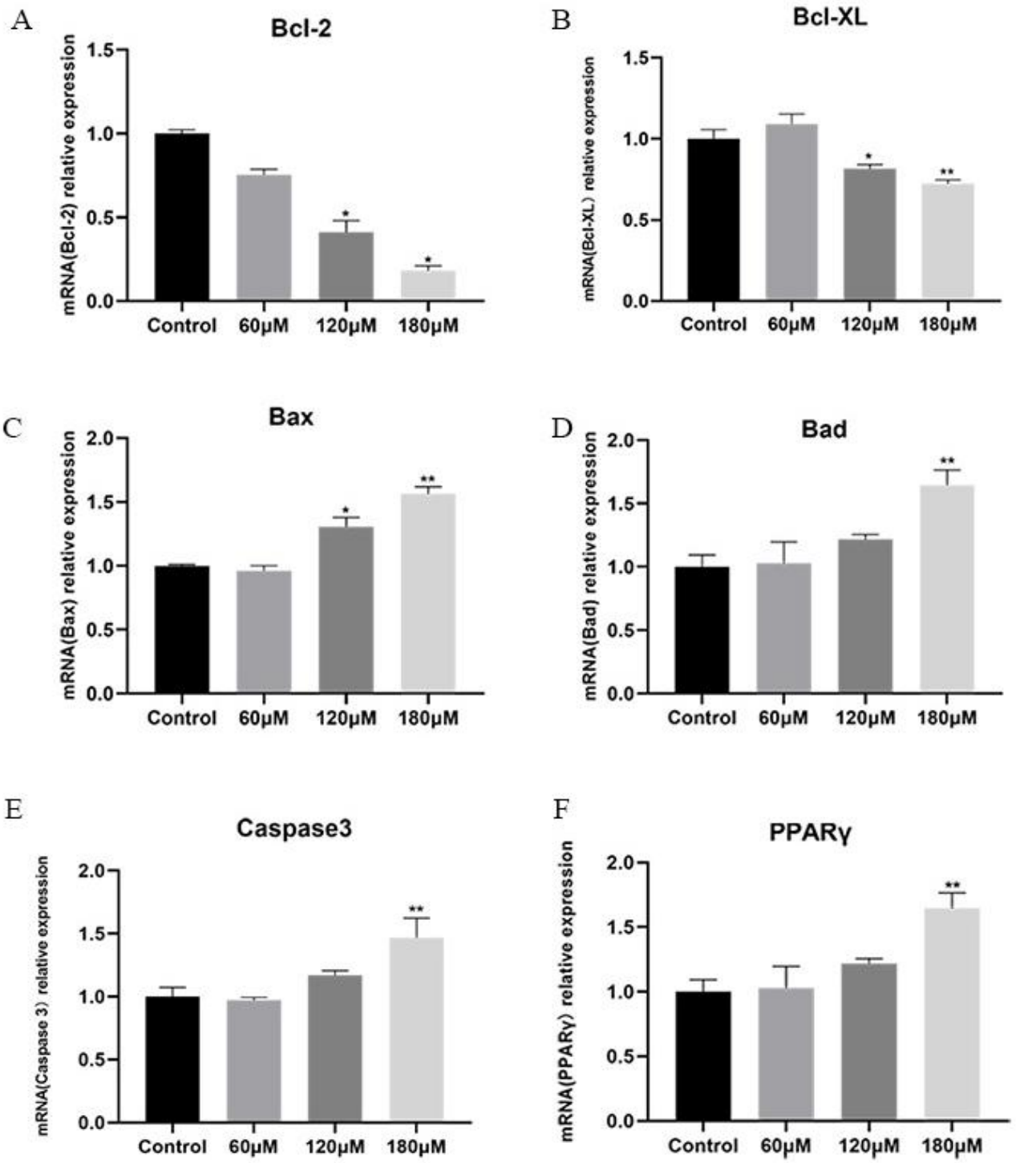

Fig.2: Detection of apoptosis-related genes induced by c9, t11-CLA at different concentrations in CMT-U27 cells. (A-B) Changes in the expression levels of the anti-apoptosis-related genes Bcl-2 and Bcl-XL; (C-D) Changes in the expression levels of the pro-apoptosis-related genes Bax and Bad; (E-F) Changes in the expression levels of the apoptosis-related genes PPARγ and caspase-3. Mean±SEM was calculated from three independent experiments. *P<0.05, **P<0.01.

significant alteration at 60μM but demonstrated a significant increase at 120 and 180μM of c9, t11-CLA (P<0.01) (Fig. 3-A, D).

Detection of antioxidant function of CMT-U27 cells mediated by c9, t11-CLA: According to what is shown in Figure 3-(E, G), the SOD activity and gene expression level of catalase (CAT), an antioxidant-related factor, gradually decreased with the increase in c9, t11-CLA concentration following the exposure of CMT-U27 cells to c9, t11-CLA. However, the malondialdehyde (MDA) content increased with increasing c9, t11-CLA concentrations. At 60μM, the SOD and CAT activity showed no significant difference from the control group, whereas the MDA content increased significantly (P<0.01). At ≥ 120μM, SOD activity decreased (P<0.05), while CAT gene expression exhibited a significant reduction (P<0.01).

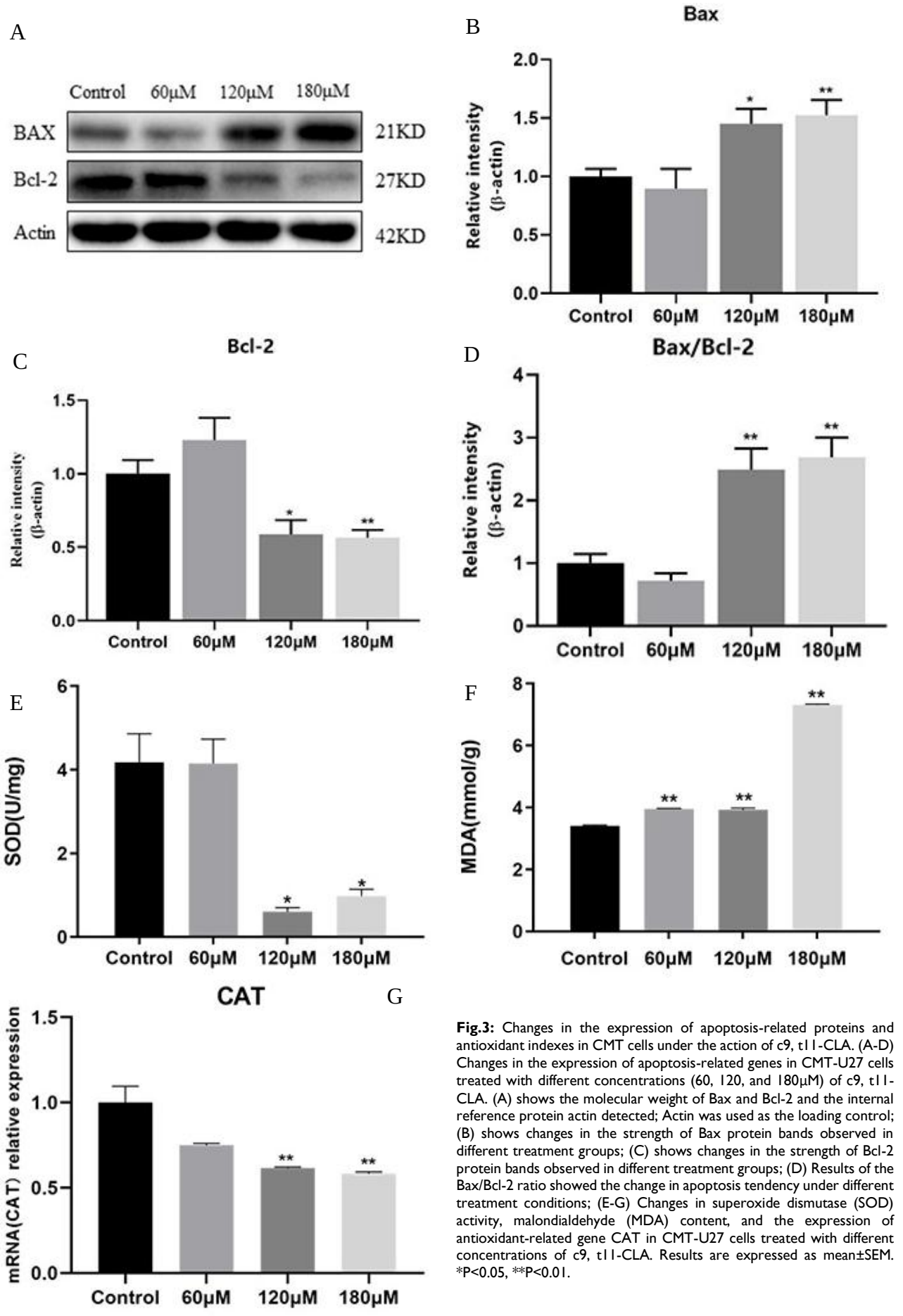

Fig.3: Changes in the expression of apoptosis-related proteins and antioxidant indexes in CMT cells under the action of c9, t11-CLA. (A-D) Changes in the expression of apoptosis-related genes in CMT-U27 cells treated with different concentrations (60, 120, and 180μM) of c9, t11-CLA. (A) shows the molecular weight of Bax and Bcl-2 and the internal reference protein actin detected; Actin was used as the loading control; (B) shows changes in the strength of Bax protein bands observed in different treatment groups; (C) shows changes in the strength of Bcl-2 protein bands observed in different treatment groups; (D) Results of the Bax/Bcl-2 ratio showed the change in apoptosis tendency under different treatment conditions; (E-G) Changes in superoxide dismutase (SOD) activity, malondialdehyde (MDA) content, and the expression of antioxidant-related gene CAT in CMT-U27 cells treated with different concentrations of c9, t11-CLA. Results are expressed as mean±SEM. *P<0.05, **P<0.01.

DISCUSSION

Studies have demonstrated that the chemically induced tumors in the mammary gland, colon, forestomach, and skin can be inhibited by dietary supplementation with CLA isomers (Hwang *et al*., 2007; Kim *et al*., 2010; Białek *et al*., 2016; Dubey *et al*., 2023). Meanwhile, it has been documented that CLA isomers exert antiproliferative effects on human colorectal and prostate cancer cells (Palombo *et al*., 2002), while Liu *et al*. (2002) proved that c9, t11-CLA induces a progressively effects of apoptosis and antiproliferation in gastric adenocarcinoma cells (SGC-7901) with an increase in c9, t11-CLA concentration, which can favor our results. According to what has been proved by Oliveira Lopes *et al*. (2024), CMTs share significant histological, clinicopathological, and molecular characteristics with human breast cancer (HBC), making them valuable comparative models for oncological research. El Roz *et al*. (2013) have confirmed that CLA can inhibit the proliferation of the HBC cell line MCF-7 and promote its apoptosis. In the present study, we used the CMT-U27 cell line to evaluate c9, t11-CLA's antiproliferation effects, revealing that the cells' morphology underwent significant changes, and the growth inhibition rate increased as c9, t11-CLA increased. In the future, we should focus on addressing the issue of tumor heterogeneity, classifying CMTs, and investigating whether differences exist in CLA on different subtypes of tumor cells.

There is increasing evidence that tumor transformation, development, and metastasis are associated with alterations in apoptotic pathways, and most chemotherapeutic agents utilize apoptotic pathways to induce cancer cell death (Tamarindo *et al*., 2016). In the current study, we used an inverted microscope to observe the morphology of the CMT-U27 cells subjected to different concentrations of c9, t11-CLA. Apoptosis is characterized by distinct morphological alterations in cells, specifically manifested as chromatin condensation, reduced cell adhesion, diminished refractility, nuclear fragmentation, and the formation of apoptotic bodies, as we detected the apoptotic changes.

As is known, the intrinsic apoptotic pathway culminates in mitochondrial outer membrane permeabilization (MOMP), mediated by oligomerization of Bax and Bak and activation of caspases. Anti-apoptotic proteins block the aforementioned effects (Lalier *et al*., 2022). Research has reported that the Bax/Bcl-2 ratio serves as a critical determinant of apoptotic susceptibility, with an elevated ratio promoting caspase-3 activation (Renault *et al*., 2013), and it has been proven that its dysregulation contributes to pathological conditions such as cancer (Zhang *et al*., 2014). In our investigation, the quantitative analysis of pro-apoptotic (Bax, Bad) and anti-apoptotic (Bcl-2, Bcl-xL) gene expression revealed that c9, t11-CLA could inhibit the expression of Bcl-2 while upregulating Bax, thereby increasing the Bax/Bcl-2 ratio and inducing caspase-3-mediated apoptosis. Collectively, these results not only confirm the observations of Yoo *et al*. (2024a) but also provide new mechanistic insights that c9, t11-CLA has the antiproliferation effects of CMTs through modulation of Bcl-2 protein family expression patterns and activation of the mitochondrial apoptosis pathway. According to the research of Da Silva *et al*. (2023a), tumor heterogeneity in CMTs critically influences apoptosis to CLA isomers, while c9, t11-CLA shows promise for tubule papillary carcinoma but not anaplastic carcinoma. While findings from a single tumor subtype provide preliminary insights, only the CMT-U27 cell line derived from a primary infiltrating ductal carcinoma (Hellmén *et al.*, 1992) may be insufficient to establish definitive conclusions. Future investigations will incorporate various subtypes to underscore the molecular heterogeneity of canine mammary neoplasia. (Edmunds *et al.*, 2023).

Furthermore, we detected the relevant expression of PPARγ, which is present at the intersection of different signal transductions and is closely related to tumorigenesis and tumor progression (Sobolev *et al*., 2025). Once activated, as reported by Lee *et al*. (2024), PPARγ can not only inhibit the proliferation but also induce the apoptosis of tumor cells. Studies have demonstrated that c9, t11-CLA induces the apoptosis of canine nasal carcinomas (Paciello *et al*., 2007) and liver cancer cells (Lu *et al*., 2015a) by activating the PPARγ signaling pathway. Our research has proven that c9, t11-CLA can induce an increased expression of PPARγ, correlating with changes in apoptotic regulatory genes such as Bax, Bcl-2, and caspase-3. Collectively, our results support the hypothesis that PPARγ activation contributes to c9, t11-CLA-induced apoptosis in CMTs, as evidenced by its association with altered expression of apoptotic regulators (Bax, Bcl-2).

Lipids represent the primary biological targets of oxidative stress (OS), with their peroxidation derivatives exhibiting the capacity to propagate and amplify oxidative damage through chain reactions. MDA is a stable biomarker of assessing lipid peroxidation, and its content is generally evaluated to quantify the level of OS (Tsikas, 2017). As an important antioxidant metalloenzyme, SOD scavenges ROS and maintains the redox homeostasis. The current investigation proved that excessive production of ROS can cause inflammation and OS through interacting with the TLR4 system (Keestra *et al*., 2013). Our results confirmed that elevated the MDA concentration was accompanied by the increased level increased serum levels of SOD when the drug concentration was at $\geq$ 120μM ($P<0.01$), indicating that the effects of c9, t11-CLA on the cells improved OS, and the ROS generated in the cells caused lipid peroxidation, thereby damaging the cells. While some variability exists in prior reports, our controlled experiments consistently support the model proposed by St Clair *et al*. (2005). The Catalase (CAT) enzyme activity can decompose H_2O_2 to produce O_2, alleviating hypoxia in the tumor microenvironment and thereby enhancing the efficiency of tumor killing. In our study, the antioxidant level of cells was evaluated by detecting the mRNA expression level of CAT in CMTs. Results showed that the transcriptional level of CAT decreased with an increasing concentration of c9, t11-CLA. However, SOD activity and CAT mRNA may not fully reflect cellular redox homeostasis. Thus, while our data suggests a potential role of c9, t11-CLA in disrupting the oxidative homeostasis in CMTs, the functional impact requires validation through comprehensive redox profiling.

While this study demonstrates c9, t11-CLA's antitumor effects on CMT-U27 cells, several limitations warrant discussion. First, the absence of healthy cell controls prevents definitive differentiation between specific cytotoxicity and general cellular stress responses. Second, while concentrations were empirically determined, IC50 values would provide more precise therapeutic indices. Third, though morphological and metabolic apoptosis markers were evaluated, direct assays (Annexin V / TUNEL) and caspase-3 cleavage verification would strengthen these findings, particularly given the imperfect correlation between caspase-3 mRNA and protein activation (Lin *et al*., 2024). Finally, while Bcl-2 modulation and PPARγ activation were observed, mechanistic studies using PPARγ antagonists are needed to establish causality. Addressing these limitations in future work will enhance the robustness of the findings.

Conclusions: C9, t11-CLA exerts an inhibitory effect on the proliferation of CMT-U27 cells by inducing apoptosis and disrupting the oxidative homeostasis, which the mechanism involves the regulation of Bcl-2 family proteins and activation of PPARγ. Additionally, c9, t11-CLA increases oxidative stress by elevating MDA levels and reducing SOD activity and CAT expression, leading to lipid peroxidation and cellular damage. Our findings suggest that c9, t11-CLA may hold therapeutic potential in CMTs, pending further in vivo and mechanistic validation.

Authors contribution: Zihan Wang conceived and designed the study executed the experiments, analyzed the samples; Yuquan Ren analyzed the data and drafted the manuscript. All authors have read and approved the final manuscript.

Acknowledgements: The authors acknowledge Dr. Xiangzhen Shen for his help with the manuscript and Dr. Meng Li for her help with the materials.

Funding information: This study was funded by the National Natural Science Foundation of China (Grant 32373087).

Conflict of interest statement: The authors declare no conflicts of interest.

Data availability statement: The data that support the findings of this study are available from the corresponding author upon reasonable request.

REFERENCES

Belury MA, 2002. Inhibition of carcinogenesis by conjugated linoleic acid: potential mechanisms of action. J Nutr 132:2995-8.

Białek A, Tokarz A, Zagrodzki P, 2016. Conjugated linoleic acids (CLA) decrease the breast cancer risk in dmba-treated rats. Acta Pol Pharm 73:315-27.

Chen Y, Xiao J, Zhu X, *et al*., 2024. Exploiting conjugated linoleic acid for health: a recent update. Food Funct 16:147-167.

Cuciniello R, Luongo D, Maurano F, *et al*., 2024. Dietary conjugated linoleic acid downregulates the $AlCl_3$-induced hyperactivation of compensatory and maladaptive signalling in the mouse brain cortex. Free Radic Biol Med 213:102-112.

Da Silva ED, Sandri EC, Fernandes LA, *et al*., 2023. Conjugated linoleic acid trans-10, cis-12 increases the expression of genes from cell cycle progression and cis-9, trans-11 stimulates apoptotic genes in different mammary tumor explants of female dogs. Mol Biol Rep 50:4011-4015.

Dubey V, Mishra AK, Ghosh AR, 2023. Appraisal of the possible role of PPARγ upregulation by CLA of probiotic *Pediococcus pentosaceus* GS4 in colon cancer mitigation. PPAR Res 2023:9458308.

Edmunds G, Beck S, Kale KU, *et al*., 2023. Associations between dog breed and clinical features of mammary epithelial neoplasia in bitches: an epidemiological study of submissions to a single diagnostic pathology centre between 2008-2021. J Mammary Gland Biol Neoplasia 28:6.

El Roz A, Bard J M, Huvelin J M, *et al*., 2013. The anti-proliferative and pro-apoptotic effects of the trans9, trans11 conjugated linoleic acid isomer on MCF-7 mammary cancer cells are associated with LXR activation. PLEFA 88: 265-272.

Fite A, Goua M, Wahle K W J, *et al*., 2007. Potentiation of the anti-tumour effect of docetaxel by conjugated linoleic acids (CLAs) in breast cancer cells in vitro. PLEFA 77:87-96.

Hellmén E, 1992. Characterization of four in vitro established canine mammary carcinoma and one atypical benign mixed tumor cell lines. In Vitro Cell Dev Biol 28A:309-19.

Hwang DM, Kundu JK, Shin JW, *et al*., 2007. Cis-9, trans-11-conjugated linoleic acid down-regulates phorbol ester-induced NF-kappaB activation and subsequent COX-2 expression in hairless mouse skin by targeting IkappaB kinase and PI3K-Akt. Carcinogen 28:363-71.

Iorizzo M, Di Martino C, Letizia F, *et al*., 2024. Production of conjugated linoleic acid (CLA) by *Lactiplantibacillus plantarum*: a review with emphasis on fermented foods. Foods 13:975.

Jensen R G, 2002. The composition of bovine milk lipids: January 1995 to December 2000. J Dairy Sci 85: 295-350.

Keestra AM, de Zoete MR, Bouwman LI, *et al*., 2013. Unique features of chicken Toll-like receptors. Dev Comp Immunol 41:316-23.

Kim YS, Kim SJ, Oh TW, *et al*., 2010. Differential inhibitory effects of conjugated linoleic acid isomers on mouse forestomach neoplasia induced by benzo(a)pyrene. J Agric Food Chem 58:3177-83.

Kristiansen VM, Peña L, Díez Córdova L, *et al*., 2016. Effect of ovariohysterectomy at the time of tumor removal in dogs with mammary carcinomas: a randomized controlled trial. J Vet Intern Med 30:230-41.

Lalier L, Vallette F, Manon S, 2022. Bcl-2 family members and the mitochondrial import machineries: the roads to death. Biomolecules 12:162.

Lee SY, Shin MJ, Choi SM, *et al*., 2024. Role of peroxisome proliferator-activated receptor α-dependent mitochondrial metabolism in ovarian cancer stem cells. Int J Mol Sci 25:11760.

Lin XX, Yang PQ, Li XJ, *et al*., 2024. Network pharmacology-based analysis and *in vitro* experimental verification of the inhibitory role of luteoloside on gastric cancer cells via the p53/p21 pathway. Oncol Lett 29:76.

Liu JR, Li BX, Chen BQ, *et al*., 2002. Effect of cis-9, trans-11-conjugated linoleic acid on cell cycle of gastric adenocarcinoma cell line (SGC-7901). World J Gastroenterol 8:224-9.

Lu G, Zhang G, Zheng X, *et al*., 2015. C9, t11- conjugated linoleic acid induces HCC cell apoptosis and correlation with PPAR-γ signaling pathway. Am J Transl Res 7:2752-63.

Machado VS, Crivellenti LZ, Bottari NB, *et al*., 2015. Oxidative stress and inflammatory response biomarkers in dogs with mammary carcinoma. Pathol Res Pract 211:677-81.

Ma N, Chang G, Huang J, *et al*., 2019. Cis-9, trans-11-conjugated linoleic acid exerts an anti-inflammatory effect in bovine mammary epithelial cells after Escherichia coli stimulation through NF-κB signaling pathway. J Agric Food Chem 67:193-200.

Mei C, Liu Y, Liu Z, *et al*., 2024. Dysregulated signaling pathways in canine mammary tumor and human triple negative breast cancer: advances and potential therapeutic targets. Int J Mol Sci 26:145.

Ngema LM, Adeyemi SA, Marimuthu T, *et al*., 2023. Short antiangiogenic MMP-2 peptide-decorated conjugated linoleic acid-coated SPIONs for targeted paclitaxel delivery in an A549 cell xenograft mouse tumor model. ACS Omega 9:700-713.

Paciello O, Borzacchiello G, Varricchio E, *et al*., 2007. Expression of peroxisome proliferator-activated receptor gamma (PPAR-gamma) in canine nasal carcinomas. J Vet Med A Physiol Pathol Clin Med 54:406-10.

Palombo JD, Ganguly A, Bistrian BR, *et al*., 2002. The antiproliferative effects of biologically active isomers of conjugated linoleic acid on human colorectal and prostatic cancer cells. Cancer Lett 177:163-72.

Park HS, Ryu JH, Ha YL, *et al*., 2001. Dietary conjugated linoleic acid (CLA) induces apoptosis of colonic mucosa in 1,2-dimethylhydrazine-treated rats: a possible mechanism of the anticarcinogenic effect by CLA. Br J Nutr 86: 549-555.

Poleti MD, Regitano LCA, Souza GHMF, *et al*., 2020. Proteome alterations associated with the oleic acid and cis-9, trans-11 conjugated linoleic acid content in bovine skeletal muscle. J Proteomics 222:103792.

Renault TT, Teijido O, Antonsson B, *et al*., 2013. Regulation of Bax mitochondrial localization by Bcl-2 and Bcl-x(L): keep your friends close but your enemies closer. Int J Biochem Cell Biol 45:64-7.

Sleeckx N, de Rooster H, Veldhuis Kroeze EJ, *et al*., 2011. Canine mammary tumors, an overview. Reprod Domest Anim 46:1112-31.

Sobolev V, Tchepourina E, Soboleva A, *et al*., 2025. PPAR-γ in melanoma and immune cells: insights into disease pathogenesis and therapeutic implications. Cells 14:534.

St Clair D, Zhao YF, Chaiswing L, *et al*., 2005. Modulation of skin tumorigenesis by SOD. Biomed Pharmacother 59: 209-214.

Tamarindo GH, Novais AA, Chuffa LGA, *et al*., 2023. Metabolic alterations in canine mammary tumors. Animals (Basel) 13:2757.

Tsikas D, 2017. Assessment of lipid peroxidation by measuring malondialdehyde (MDA) and relatives in biological samples: analytical and biological challenges. Anal Biochem 524:13-30.

Wang L S, Huang Y W, Sugimoto Y, *et al*., 2006. Conjugated linoleic acid (CLA) up-regulates the estrogen-regulated cancer suppressor gene, protein tyrosine phosphatase gamma (PTPgama), in human breast cells. Anticancer Res 26: 27-34.

Wu L, Ye S, Deng X, *et al*.,2024. Conjugated linoleic acid ameliorates high fat-induced insulin resistance via regulating gut microbiota-host metabolic and immunomodulatory interactions. Nutrients 16:1133.

Yoo MJ, Jang YJ, Park SY, *et al*., 2024. Synergistic anti-cancer effects of ERB-041 and genistein through estrogen receptor suppression-mediated PI3K/AKT pathway downregulation in canine mammary gland tumor cells. Int J Mol Sci 25:2466.

Zeng Y, Liu P, Yang X, *et al*., 2020. The dietary c9, t11-conjugated linoleic acid enriched from butter reduces breast cancer progression in vivo. J Food Biochem 44:e13163.

Zhang X, Bi L, Ye Y, *et al*., 2014. Formononetin induces apoptosis in PC-3 prostate cancer cells through enhancing the Bax/Bcl-2 ratios and regulating the p38/Akt pathway. Nutr Cancer 66:656-61.